

A Fuzzy IRFOC Application Based Speed Sensorless Control of Induction Machine Using a Speed and Load Torque Observer

K. Abed, K. Nabti and H. Benalla

Department of Electrical Engineering, Faculty of Engineering Sciences,
 Mentouri University Route d'Ain El Bey, Constantine, Algeria

Abstract: In this study, a Fuzzy controller of an Indirect Rotor Field Oriented Control (IRFOC) using a speed observer for an Induction Machine (IM) drive, feed through an ameliorate voltage inverter is proposed. A superiority of the proposed fuzzy controller over conventional PI controller in handling nonlinear such as an induction motor has been effectively demonstrated by comparing F-PI speed controller with the conventional PI under varying operating conditions like step change in speed reference and torque reference. Observers use a model to predict the speed by the phase currents and voltages as state variables, these estimates are improved by an error feedback compensator that measures the difference between the estimated and actual values. The observed value of speed is then used by the FOC to adjust the PWM waveform in exactly the same way as an actual measured value.

Key words: IRFOC, sensorless control, Induction Machine (IM), ameliorate three level voltage inverter, PWM, Fuzzy-PI (F-PI) controller, Luenberger observer, simulink

INTRODUCTION

Induction motors are widely used in industrial applications because they are less cost, more rugged and reliable than DC motors. Though induction motors have a few advantageous characteristics, they possess nonlinear and time-varying dynamic interactions. Using conventional PI controller, it is very difficult and complex to design a high performance induction motor drive system.

The fuzzy logic controller is attractive approach, which can accommodate the motor parametric variations and difficulty in obtaining an accurate mathematical model of induction motor due to rotor parameter and load time constant variations. In order to have fast transient response, the controller must have the robustness against speed variations and external perturbations. The fuzzy logic is applied to optimize the PI controller gains which designed to optimize the step response of the system.

In this study, we describe the speed control strategies of an IRFOC for IM. Next, with help of the Matlab/Simulink, we propose the F-PI controller, which is suitable for speed control without mechanical sensors, an observer is used for predict the load torque and speed. Finally, we compare the F-PI simulation results to conventional proportional-plus integral controller. The

simulation results validate the robustness and reliable of the proposed F-PI controller for high performance of induction motor drive.

THREE LEVEL VOLTAGE INVERTER

As for the two level voltage inverters, we can produce a three-phase three level voltage inverter in complete bridge by assembling three half-bridges using a common capacitive divider (Fig. 1).

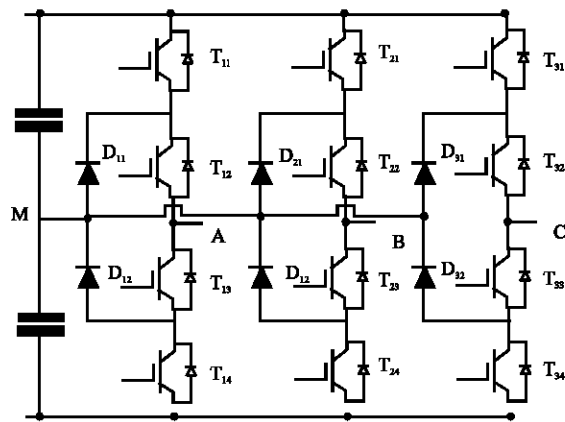


Fig. 1: Three level neutral-point-clamped inverter circuit

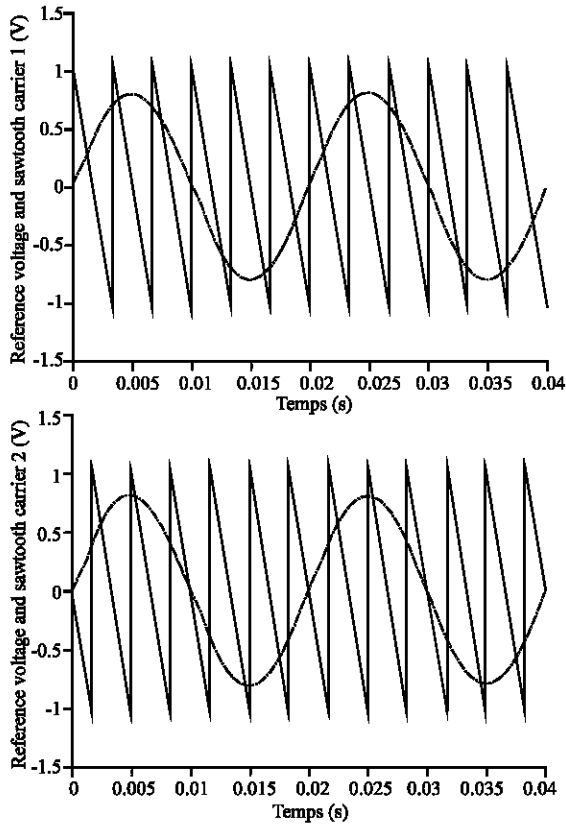


Fig. 2: Principel of sawtooth-sinusoidal command with two carriers

Different PWM strategies to control the three level voltage inverter are given in *Abed et al.* (2006) we use the Sawtooth-Sinusoidal command with two carriers. This strategy is defined by two identical carriers, which one is delay compared to the other by a half-period (Fig. 2).

FIELD ORIENTED CONTROL STRUCTURE

A block diagram for an IRFOC can be seen on Fig. 3. This design uses a more robust structure known as Indirect Rotor Field Oriented Control, meaning that the rotor angle isn't determined directly by measuring the air gap flux with hall-effect sensors. These sensors are not particularly suited for use in large industrial motors as they can be fragile and sensitive to temperature change (*Abed et al.*, 2006 b; *Rajashekara et al.*, 1996).

The dynamic model of an induction motor can be represented according to usual d-q axes components in asynchronous rotating frame as follows:

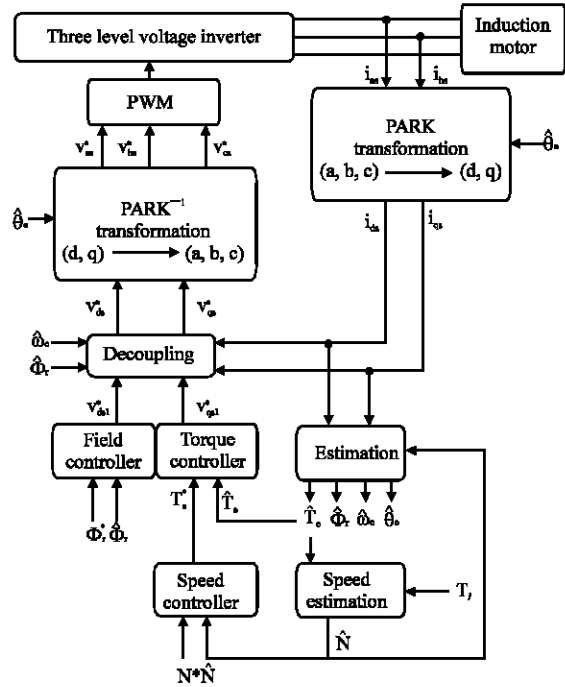


Fig. 3: Field oriented controller block diagram (*Abed et al.*, 2006b)

$$\begin{bmatrix} \frac{di_{ds}}{dt} \\ \frac{di_{qs}}{dt} \\ \frac{d\phi_{dr}}{dt} \\ \frac{d\phi_{qr}}{dt} \end{bmatrix} = \begin{bmatrix} -\gamma & \omega_e & \frac{k}{\tau_r} & N_p N k \\ -\omega_e & -\gamma & -N_p N k & \frac{k}{\tau_r} \\ \frac{L_m}{\tau_r} & 0 & -\frac{1}{\tau_r} & \omega_e - N_p N \\ 0 & \frac{L_m}{\tau_r} & -(\omega_e - N_p N) & -\frac{1}{\tau_r} \end{bmatrix} \begin{bmatrix} i_{ds} \\ i_{qs} \\ \phi_{dr} \\ \phi_{qr} \end{bmatrix} + \begin{bmatrix} \frac{1}{\sigma L_s} & 0 \\ 0 & \frac{1}{\sigma L_s} \\ 0 & 0 \\ 0 & 0 \end{bmatrix} \begin{bmatrix} v_{ds} \\ v_{qs} \end{bmatrix} \quad (1)$$

Where:

$$\sigma = 1 - \frac{M^2}{L_s L_r}, \quad \tau_r = \frac{L_r}{R_r}$$

The decoupling control between d and q axes can be achieved by aligning the rotor flux vector to the d-axis and setting the rotor flux linkage to be constant, which means:

$$\Phi_{qr} = \frac{d\Phi_{qr}}{dt} = 0 \quad (2)$$

$\Phi_{dr} = \Phi_r = \text{rated flux}$

Substituting (2) in (1) yields:

$$\begin{cases} v_{ds} = \sigma L_s \frac{di_{sd}}{dt} + \left(R_s + R_r \frac{M^2}{L_r^2} \right) i_{ds} - \omega_e \sigma L_s i_{qs} - \frac{M}{L_r} R_r \Phi_r \\ v_{qs} = \sigma L_s \frac{di_{sq}}{dt} + \omega_e \sigma L_s i_{sq} + \left(R_s + R_r \frac{M^2}{L_r^2} \right) i_{ds} - \frac{M}{L_r} N_p N \Phi_r \\ \tau_r \frac{d\Phi_r}{dt} + \Phi_r = M i_{ds} \\ \omega_e = N_p N + \frac{M}{\tau_r} \frac{i_{qs}}{\Phi_r} \end{cases} \quad (3)$$

The electromagnetic torque equation and the mechanical speed motor are related by:

$$J \frac{dN}{dt} + fN = T_e - T_l \quad (4)$$

Where, the electromagnetic torque equation is:

$$T_e = N_p \frac{M}{L_r} \Phi_r i_{qs} \quad (5)$$

The decoupling control system is given by:

$$\begin{cases} v_{ds}^* = v_{ds1} - e_{ds} \\ v_{qs}^* = v_{qs1} - e_{qs} \end{cases} \quad (6)$$

Where:

$$\begin{cases} e_{ds} = \hat{\omega}_e \sigma L_s i_{qs} + \frac{M}{L_r} R_r \Phi_r \\ e_{qs} = -\hat{\omega}_e \sigma L_s i_{ds} - \frac{M}{L_r} \hat{\omega}_e \Phi_r + \frac{M^2}{L_r \tau_r} i_{qs} \end{cases} \quad (7)$$

DESIGN OF F-PI CONTROLLER FOR INDUCTION MOTOR

The purpose of this study, is to synthesize a controller without the exact knowledge of a model, numerically simple and simulated on Matlab/Simulink allowing good performance in terms of overshoot and fast and accuracy under the speed and load variations. The Fuzzy Logic Toolbox based controller architecture is shown in Fig. 4.

The fuzzy logic controller employs speed error and change of speed error as inputs, the reference torque is output.

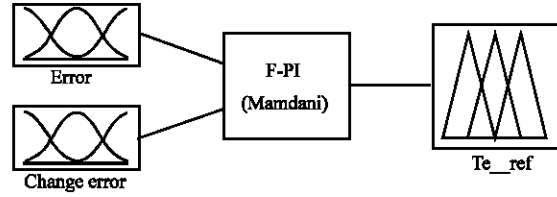


Fig. 4: Fuzzy controller architecture

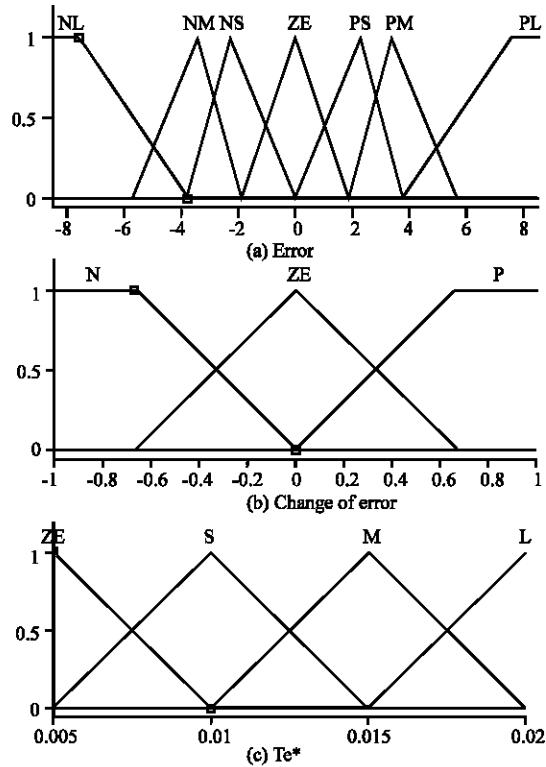


Fig. 5: Membership function of input, output variables

$$e(k) = N - \hat{N} \quad (8)$$

$$\Delta e(k) = e(k) - e(k-1) \quad (9)$$

And it uses following linguistic labels: {NL (Negative Large), NM (Negative Medium), NS (Negative Short), ZE (Zero), PS (Positive Short), PM (Positive Medium), PL (Positive Large)}. Each fuzzy label has an associated membership function. The membership functions as shown in Fig. 5.

The control rules are represented as a set of if then rules. The fuzzy rules of proposed controller for speed control of induction motor are presented in Table 1. And formulated as follows:

If $e(k)$ is NL and $\Delta e(k)$ is N then $Te^*(k)$ is ZE.

Table 1: Control rule base

E/CE	NL	NM	NS	ZE	PS	PM	PL
N	ZE	S	M	L	M	S	ZE
ZE	ZE	S	M	L	M	S	ZE
P	ZE	M	L	L	L	M	ZE

The present study uses Mamdani's Max-Min algorithm for inference mechanism. In the defuzzification stage, a crisp value of the output variable is obtained by using the center of gravity method.

$$\Delta\mu_0 = \frac{\sum_{j=0}^n C^0(\Delta\mu_j) \Delta\mu_j}{\sum_{j=0}^n C^0(\Delta\mu_j)} \quad (10)$$

SENSORLESS SPEED CONTROL ALGORITHM

Synchronous angular speed estimation (Pinard, 2004; Abed et al., 2007): From the row 4 of (3) we obtain

$$\omega_e = N_p N + \frac{M}{\tau_r} \frac{i_{qs}}{\Phi_r + \varepsilon} \quad (11)$$

Car $\Phi_r = 0$ in $t = 0$ s

Where: $\hat{\Phi}_r$ is the estimate flux, $\varepsilon = 0.01$.
From the row (3):

$$\hat{\Phi}_r = \frac{M}{1 + \tau_r p} i_{ds} \quad (12)$$

Once we obtain the synchronous angular speed, θ_e is simply equal to:

$$\theta_e = \int \omega_e \quad (13)$$

Knowledge of the synchronous angular speed and θ_e is essential for accurately applying the Clarke and Park transforms.

Speed control: Sensorless control is another extension to the IRFOC algorithm that allows IMs to operate without the need for mechanical speed sensors. These sensors are notoriously prone to breakage, so removing them not only reduces the cost and size of the motor but improves the drive's long term accuracy and reliability (Chavez et al., 2004; Lysherski, 2000; Shi et al., 2000; Shoudao et al., 2004). This is particularly important if the motor is being used in a harsh, inaccessible environment such as an oil well (Fig. 6).

Instead of physically measuring certain values control engineers can calculate them from a system's state

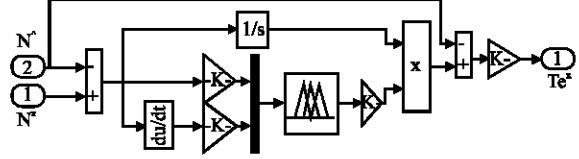


Fig. 6: Simulink model of fuzzy controller for IM

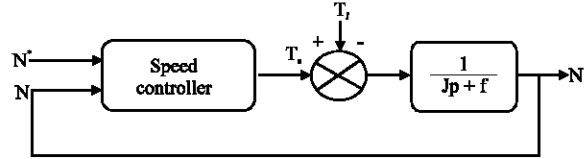


Fig. 7: Block diagram-estimation of speed

variables. This is known as the state space modeling approach and is a powerful method for analyzing and controlling complex non-linear systems with multiple inputs and outputs.

From expression (4) we establish the following transfer function

$$N = \frac{1}{Jp + f} (T_e - T_l) \quad (14)$$

In the goal of compare, we study a PI controller for a speed regulation:

$$N = \frac{1}{Jp + f} \left(\frac{K_{ps}p + K_{is}}{p} \right) (\hat{N} - N) - \frac{1}{Jp + f} T_l \quad (15)$$

Or

$$N = \frac{K_{ps}p + K_{is}}{Jp^2 + (K_{ps} + f)p + K_{is}} \hat{N} - \frac{p}{Jp^2 + (K_{ps} + f)p + K_{is}} T_l \quad (16)$$

We obtain the block diagram shows in Fig. 7.

The controller parameters of this 2nd order dynamic characteristic equation are given from:

$$\frac{J}{K_{is}} = \frac{1}{\omega_n^2}, \quad \frac{2\xi_s}{\omega_n} = \frac{K_{ps} + f}{K_{is}} \quad (17)$$

Closed loop observer implantation: The objective here is to use a load torque and speed observer in order to delete all mechanical sensors.

From (4) and (5)

$$\frac{dN}{dt} = -\frac{f}{J}N + \frac{N_p M \Phi_r i_{qs}}{JL_r} - \frac{1}{J}T_l \quad (18)$$

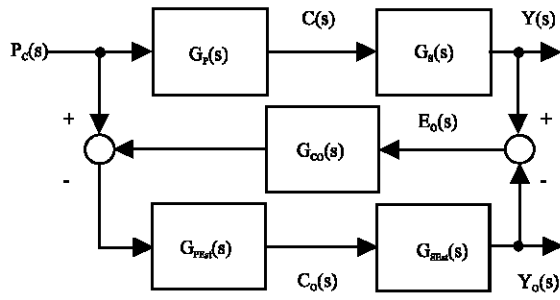


Fig. 8. The Luenberger observer (George, 2002)

The system of the 2nd order Luenberger observer (Fig. 8) is given by Ghosn (2001):

$$\begin{cases} \dot{\hat{X}} = A\hat{X} + BU + L(Y - \hat{Y}) \\ \hat{Y} = C\hat{X} \end{cases} \quad (19)$$

With:

$$\hat{X} = \begin{pmatrix} N_{obs} \\ T_1 \end{pmatrix}; L = \begin{pmatrix} l1 \\ l2 \end{pmatrix} \quad (20)$$

We have finally:

$$\begin{pmatrix} \frac{dN_{obs}}{dt} \\ \frac{dT_{1_obs}}{dt} \end{pmatrix} = \begin{pmatrix} -\frac{f}{J} - l1 & -\frac{1}{J} \\ -l2 & 0 \end{pmatrix} \begin{pmatrix} N_{obs} \\ T_{1_obs} \end{pmatrix} + \begin{pmatrix} \frac{N_p M \Phi_r}{J L_r} \\ 0 \end{pmatrix} (i_{qs}) + \begin{pmatrix} l1 \\ l2 \end{pmatrix} N \quad (21)$$

The factors l1 and l2 are selected to fix the observer dynamics, we put: l1 = 250, l2 = -600

RESULTS AND DISCUSSION

The SIMULINK model used in this study, models the induction motor as a continuous system for its dynamic equivalent circuit. The IGBT three level (NPC) inverter is controlled by a PWM with a switching frequency of 18 kHz.

We have tested the robust controller for sensorless speed controlled induction motor drive, with load torque applied as the following way

- - 10 N.m in 1.5 s.
- - 10 N.m in 2.5 s.
- +10 N.m in 6 s.
- - 10 N.m in 7 s.
- 0 N.m in 8 s.

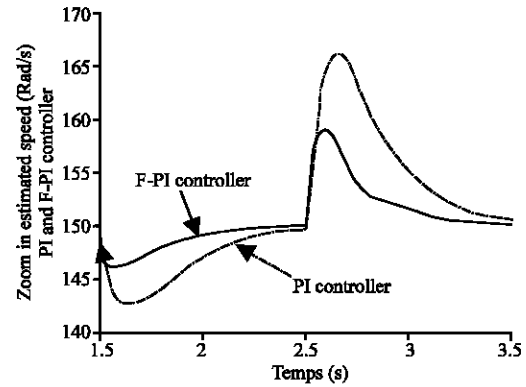


Fig. 9: Simulation results IRFOC closed loop control: Zoom in estimated speed: PI and fuzzy-PI controller

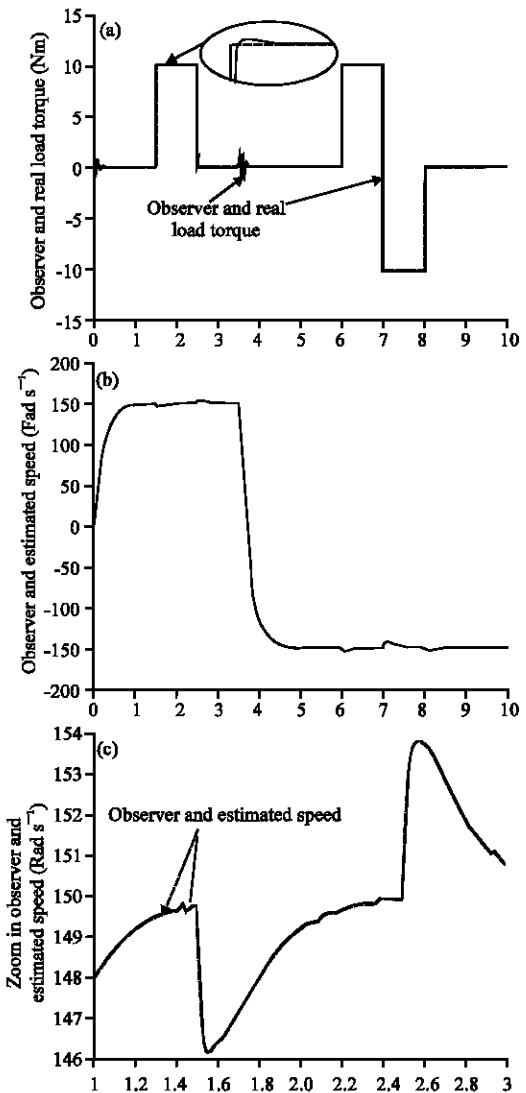


Fig. 10: Simulation results IRFOC closed loop observer implementation

For a field reference $\hat{\Phi}_r = 0.8$ Wb. The speed is fixed at 150, then -150 Rad/s into 3.5 s.

The simulation results show the superiority of the F-PI compared to the traditional PI very used in industry. Therefore, it remains the good choice, it able to reacted positively with an ameliorate three level inverter to control the IM (Fig. 9).

Figure 10 shows the speed graph of Closed Loop Observer Implantation flow the estimated speed given in §6.2, the comparaisn between the observed load torque and the real one reveals that the observation is satisfactory even if there is a difference between these two torques at the time of the transitory modes such as speed or load change.

- Observed and real load torque.
- Observed and estimated speed.
- Zoom in observed and estimated speed.

CONCLUSION

In this study, we presented the states variations in an objective of ameliorate the IM sensorless speed control by an F-PI regulator. A comparison between the F-PI controller and the conventional PI controller reveals the superiority of the first one. The fuzzy controller is less sensitive to the system parameters variation and this proves its robustness.

Nomenclature:

V_{ds}, V_{qs}	: d-q axis stator applied voltages.
i_{ds}, i_{qs}	: d-q axis stator currents.
Φ_{dr}, Φ_{qr}	: d-q rotor flux linkage.
R_s, R_r	: Stator and rotor winding resistances.
L_s, L_r	: Stator and rotor.
M	: Mutual magnetizing inductances.
N_p	: Number of pole pairs.
p	: Laplace operator.
ω_s, ω_r	: Synchronous and electrical angular speed.
T_e, T_l	: Electromagnetic and load torque.
J	: Total inertia.
f	: Friction coefficient.
τ_r	: Rotor time constant.
σ	: Leakage coefficient.
$\hat{}$: Denotes the estimated value.
\ast	: Denotes the reference value.
N, N_{obs}	: Estimated and observed speed.
$T_{l_{obs}}$: Observed load torque.

REFERENCES

- Abed, K., K. Nabti and H. Benalla, 2007. A fuzzy IRFOC application in speed sensorless control of IM supplied from an ameliorate inverter. Proceedings of the 16th IASTED International Conference Applied Simulation and Modelling, Palma de Mallorca, Spain, (581-025).
- Abed, K., K. Nabti and H. Benalla, 2006. A speed sensorless control for triphase induction machine using indirect field-oriented control scheme. Proceedings of the 15th IASTED International Conference Applied Simulation and Modelling, Rhodes, Greece (522-057), pp: 346-351.
- Abed, K., K. Nabti and H. Benalla, 2006. Ameliorate speed sensorless control of Induction Machine (IM) by a three level voltage inverter using Indirect Rotor Field Oriented Control (IRFOC) scheme, simulation and experimentation validation. Second International Conference on Electrical Systems ICE, Oum El Bouaghi, Algeria, pp: 260-265.
- Chavez, V.S., R.A. Palomares and A.N. Segura, 2004. Speed estimation for an induction motor using the extended kalman filter, electronics, communications and computers. Conielectomp. 14th International Conference, pp: 63-68.
- Ghosn, R., 2001. Contrôle vectoriel de la machine asynchrone à rotor bobiné à double alimentation, thesis for a doctoral degree. LEEI-Inseeiht, Toulouse.
- George Ellis Danaher Corporation, 2002. Observers in Control Systems a Practical Guide. Academic Press, USA.
- Lysherski, S., 2000. Electromechanical systems, electric machines and applied mechatronics. CRC Press, Boca Raton.
- Pinard, M., 2004. Commande électronique des moteurs électriques, Editions DUNOD, Paris.
- Rajashekara, K., A. Kawamura and K. Matsuse, 1996. Sensorless control of AC motor drives-speed and position sensorless operation. IEEE Press, New York.
- Shi, K.L., T.F. Chan, Y.K. Wong and S.L. Ho, 2000. Speed Estimation of an Induction Motor Drive Using Extended KALMAN Filter, Power Engineering Society Winter Meeting. IEEE., 1: 243-248.
- Shoudao, H., W. Yaonan, G. Jian, L. Jiantao and Q. Sihai, 2004. The Vector Control Based On MRAS Speed Sensorless Induction Motor Drive, Intelligent Control and Automation, WCICA. Fifth World Congress, 5: 4550-4553.